Progress In Electromagnetics Research, PIER 76, 183–194, 2007

ABMR ICE THICKNESS MODEL AND ITS APPLICATION TO BOHAI SEA IN CHINA

Y. Ji, J. Zhang, and J. Meng

First Institute of Oceanography of State Oceanic Administration
6 Xianxialing Rd., Hi-Tech Industry Park, Qingdao 266061, China

Y. Zhang

Institute of Space and Earth Information Science
Chinese University of Hong Kong
Esther Lee Building, Shatin, NT, Hong Kong

Abstract—A non-coherent theoretical model of sea-ice thickness with air-borne microwave radiometer (ABMR) was deduced based on the analysis of air-ice-water three-layer media. In the model, the high-order item of the brightness temperature was expressed and obtained. From the analysis of the penetration depth of sea-ice and its high-order item in the model, we found that ABMR with a wavelength can only be used to detect a certain range of sea-ice thickness. The maximum detectable sea-ice thickness is dependent on wavelength and precision of ABMR, whereas the minimum detectable sea-ice thickness is only related to wavelength. On this basis, the detectable sea-ice thicknesses of ABMR were calculated. The results were given on the selection of suitable ABMRs in different sea-ice conditions when ABMR is used to detect the ice thickness in Bohai Sea.

1. INTRODUCTION

Bohai Sea and northern Yellow Sea are normally ice-covered in the winter in China. This sea-ice directly affects on marine resources survey (e.g., near-shore oil-drilling operations) and sea communication transportations. The appearance of sea-ice can result in sea-ice hazard. It may also provide the latent fresh water resources [1, 2]. The sea-ice thickness is a key parameter in the estimation of the ice resources' quantity and the definition of sea-ice level. Therefore, the sea-ice thickness monitoring and its forecast are of great importance to the

sea communication and the marine work in the winter, and are most instructive to the sea-ice resources exploitation.

Sea-ice thickness in a large area can be detected with remote sensing technology [3–7]. Drucker et al. used AVHRR data to derive the ice thickness of the St. Lawrence Island [5]. But the visible/infrared image is limited to cloud-free conditions. Martin et al. retrieved the thin ice thickness with Special Sensor Microwave/Imager (SSM/I) [6], and they also estimated the ice thickness in the Chukchi Sea with AMSR-E data [7]. Compared with the space-borne microwave radiometer, the air-borne microwave radiometer (ABMR) has the advantage of flexibility, rapid response, and the higher spatial resolution. It can be used to detect ice thickness in local areas. In China, research on the ice thickness detection with ABMR has been studied. There are some kinds of ABMR with different wavelengths developed in the past two decades. Some detection experiments of ice thickness in Bohai Sea have also been carried out [8–12]. But systematic and quantitative analyses are still needed on ice thickness detectability of those ABMRs and their application ranges.

In this study, the measuring wavelength range of ABMR is quantitatively investigated on the basis of sea-ice thickness theoretical model. The selection of wavelengths is also discussed when ABMR is applied to measure the ice thickness in Bohai Sea.

2. SEA ICE THICKNESS INVERSION MODEL

A three-layer-model is established in this study. It consists of air, sea ice and sea water. Fig. 1 shows the schematic diagram with an exterior radiation source. Based on the non-coherent theory, the absorptivity of the sea-ice could be calculated as the electromagnetic energy attenuates

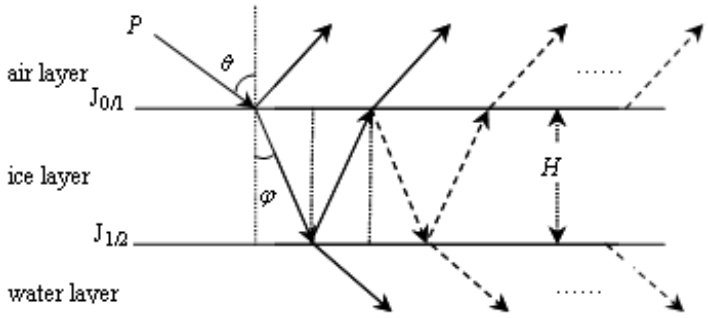

Figure 1. The schematic diagram of three-layer system with an exterior radiation source.

exponentially with the increasing of the media depth [13]. According to Kirchhoff's law [14], the emissivity of the ice layer is equal to its absorptivity. That is, the bright temperature of the air-born microwave radiometer can be calculated. Fig. 2 gives the schematic diagram without an exterior radiation source. Therefore, the energy received by the radiometer (Fig. 2) came from two parts: one is from sea-ice layer and the other is from sea water layer.

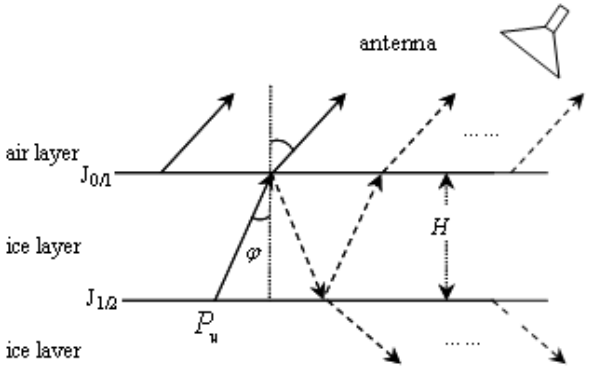

Figure 2. The schematic diagram of ABMR.

Assuming that the temperature of the sea water is equal to the sea-ice temperature, the bright temperature of ABMR could be expressed as follows

$$T_b = [1 - r_{0/1} - \left(1 - r_{0/1}\right)^2 r_{1/2} e^{-2KaH\sec\varphi}]T_1 + \Delta G T_1 \qquad (1)$$

where T_b is the bright temperature obtained by the AMBR antenna, T_1 is the physical temperature of the ice layer and water (K); $r_{0/1}$ and $r_{1/2}$ is the reflectivity of the interface $J_{0/1}$ and $J_{1/2}$, respectively, which can be calculated by the Fresnell law [14]; ΔG refers to the high-order item of bright temperature with the formula as

$$\Delta G = -\frac{e^{4KaH\sec\theta} r_{0/1}\left(1 - r_{0/1}\right)^2 r_{1/2}^2}{1 - A^2 r_{0/1} r_{1/2}} < 0 \qquad (2)$$

where H is the ice thickness; θ is the angle of reflection in the ice layer; Ka is the attenuation coefficient obtained from $Ka = \delta/2$; δ means the penetration depth of electromagnetic wave into the ice, which is defined as the propagation length when the energy of the electromagnetic wave attenuates to $1/e$, with the value of $\delta = \frac{\lambda}{2\pi}\frac{\sqrt{\varepsilon'}}{\varepsilon''}$. Where, λ is wavelength of the microwave radiometer, ε' and ε'' are real part and imaginary part, respectively, of the sea-ice dielectric constant.

If the high-order item $\Delta G T_1$ is omitted, the solid line energy will only be taken into account in the model

$$T_b = [1 - r_{0/1} - \left(1 - r_{0/1}\right)^2 r_{1/2} e^{-2KaH \sec\theta}]T_1 \tag{3}$$

Then the empirical formula of the sea-ice thickness can be written as

$$T_b = a - be^{-cH} \tag{4}$$

where a, b and c are non-negative coefficients. They can be obtained from the regression of the measured sea-ice thickness and the bright temperature in ABMR. Therefore, the sea-ice thickness can be calculated from the bright temperature of ABMR as follows

$$H = \frac{1}{c} \ln\left(\frac{b}{a - T_b}\right) \tag{5}$$

3. MEASURING RANGE OF SEA-ICE THICKNESS IN ABMR

3.1. High Limit of Ice Thickness Measuring Range

It can be noted that the bright temperature T_b in Eq. (3) received by ABMR is dependent on the ice temperature T_1, the ice thickness H, the reflectivity r, incidence angle φ, and the ice penetration depth δ. If the ice characteristics and environmental conditions is stable (e.g., T_1, r, θ fixed), the changes of the bright temperatures in two ABMRs with different wavelengths and the ice thickness will be shown in Fig. 3. Where, H_1 and H_2 are the ice thicknesses retrieved from the approximation model if two ABMRs of different wavelengths were used to detect the ice thickness.

Figure 3 also shows that the bright temperature gradually increases with the increase of ice thickness and is toward a fixed value $T_{b\max}$ (i.e., $t_{0/1}T_1$). When the difference of T_b and $T_{b\max}$ is less than ΔT, ABMR cannot distinguish the changes of the bright temperature if ice thickness continues to increase. In this case, it is not suitable to retrieve sea-ice thickness using Eq. (1). For this reason, when T_B is equal to $(1 - r_{0/1})T_1 - \Delta T$, the capability of ABMR to detect sea-ice thickness is highly limited. Its maximal detectable ice thickness is $H_{\max}$. From Eq. (3), it can be expressed as

$$H_{\max} = \frac{\delta \cos\theta}{4} \ln\left(\frac{\left(1 - r_{0/1}\right)^2 r_{1/2} T_1}{\Delta T}\right) \tag{6}$$

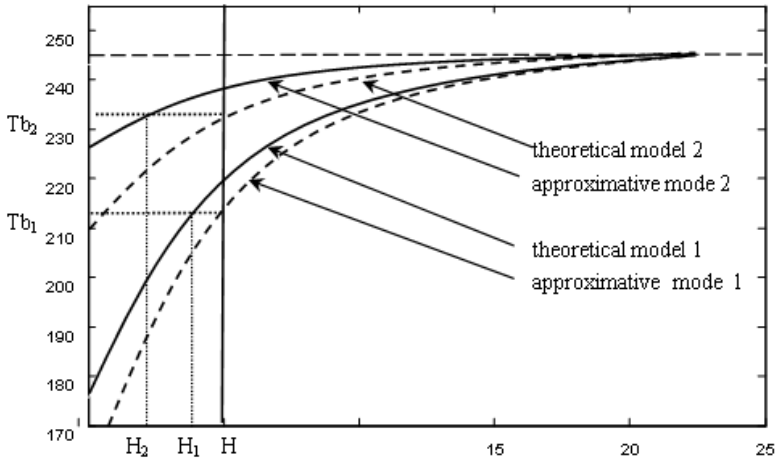

Figure 3. The scatter curve of the bright temperature with the ice thickness.

when the incidence angel θ is 0°, $\cos\theta$ is equal to 1. The reflectivity r can be obtained from Kirchhoff's law, $e = 1 - r$, and e is emissivity. Thus Eq. (6) can be written as

$$H_{\max} = \frac{\delta}{4} \ln \left(\frac{e_{0/1}^2 \left(1 - e_{1/2}\right) T_1}{\Delta T} \right) \tag{7}$$

The emissivity of sea-ice and sea water is $0.8 \sim 0.95$ and $0.23 \sim 0.63$, respectively, and both of them increase with the frequency [15]. Since the variation ranges of $e_{0/1}$ and $e_{1/2}$ are relatively small, the effects of the precision of ABMR on the detectable ice thickness are mainly considered. Therefore, the maximal value of $e_{0/1}$, the minimal value of $e_{1/2}$, and the ice freezing point $T_1 = 273$ were used in the model. Then Eq. (7) becomes

$$H_{\max} = \frac{\delta}{4} \ln \left(\frac{0.95^2 \times (1 - 0.23) \times 273}{\Delta T} \right) = \frac{\delta}{4} \ln \left(\frac{191}{\Delta T} \right) \tag{8}$$

It is clear that the maximal detectable ice thickness $H_{\max}$ increases as the ice penetration depth δ is increasing. It is also affected by the precision of ABMR ΔT. The higher the precision is, the higher $H_{\max}$ is.

On the other hand, Eq. (3) shows that the penetration depth of electromagnetic wave δ is mainly dependent on the ice dielectric

constant, while the ice dielectric constant changes with the salinity, temperature and density of sea ice. Ulaby [16] have carried out a thorough research on penetration depth of ice and given the penetration depth distribution maps of different types of ice with the frequency (see Fig. 4). Shaded areas correspond to the values range of dielectric constant commonly reported in literature.

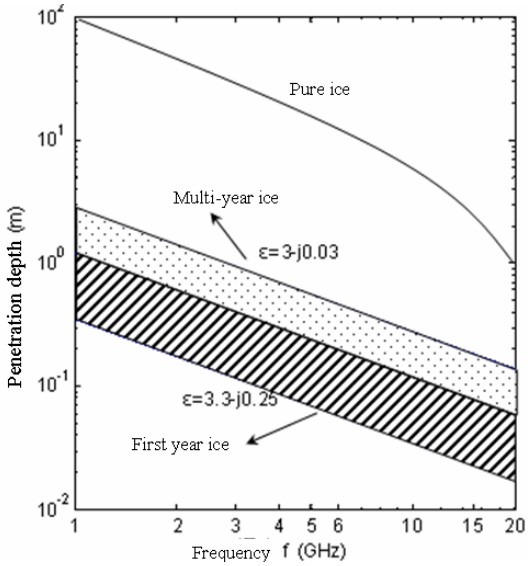

Figure 4. The ice penetration depth (from Ulaby, 1986).

When ABMRs with different wavelengths were used to detect the first year ice thickness with the precision from $1\,\mathrm{K} \sim 0.001\,\mathrm{K}$, their maximal detectable ice thickness distributions were shown in Fig. 5. Table 1 gives the list of the maximal detectable ice thicknesses at the precisions of 1 K, 0.1 K, 0.01 K, and 0.001 K. Table 2 is the list of the high-order items of ABMRs with different wavelengths at the precision of 1 K. It shows that the high-order item near at maximal detectable ice thickness is much smaller than the precision of ABMR, and thus its value can be omitted.

3.2. Low Limit of Ice Thickness Measuring Range

Figure 3 shows that the high-order item increases when the ice thickness decreases. Since the difference of the approximation curve and the theoretical curve ΔTb is large, it cannot be ignored in the model. The bright temperature in the approximation model is higher

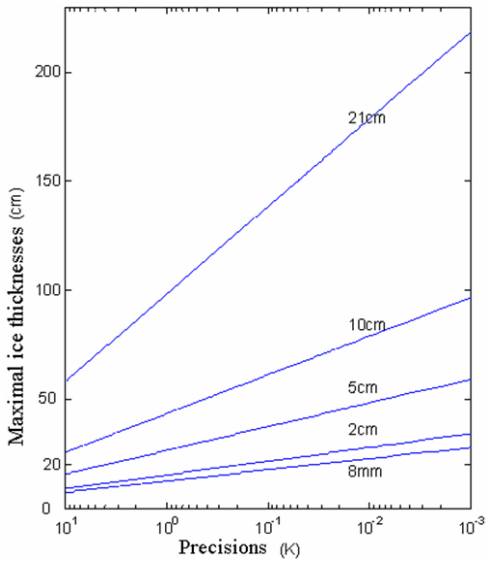

Figure 5. The maximal detectable ice thickness.

Table 1. The maximal detectable ice thicknesses of ABMR.

wavelength (frequency f)		8mm	2cm	5cm	10cm	21cm
maximal detectable ice thicknesses (cm)	ΔT=1K	12	15	25	41	92
	ΔT=0.1K	17	21	36	59	132
	ΔT=0.01K	22	27	47	77	173
	ΔT=0.001K	28	34	58	95	213

Table 2. The high-order item of the maximal ice thickness.

wavelength (frequency f)	8mm	2cm	5cm	10cm	21cm
Maximal detectable ice thickness (ΔT=1K)	12	15	25	41	92
High-order item ΔG (K)	0.0004	0.00039	0.00057	0.00054	0.00058

than that in the theoretical model at the same thickness, so the ice thickness retrieved from the approximation model is lower than its real value.

$$H_1 < H, \qquad H_2 < H \tag{9}$$

when the measurement error ΔTb was limited in an appropriate range $\Delta Tb_{\max}$, the real ice thickness $H_{\min}$ in that case was defined as the low limit ice thickness that the ABMR can detect. So the model has

not only the high limit of ice thickness $H_{\max}$, but also the low limit of ice thickness $H_{\min}$. The range between $H_{\min}$ and $H_{\max}$ can be defined as the suitable measuring range of ice thickness using ABMR

$$H_{\min} \leq H \leq H_{\max} \tag{10}$$

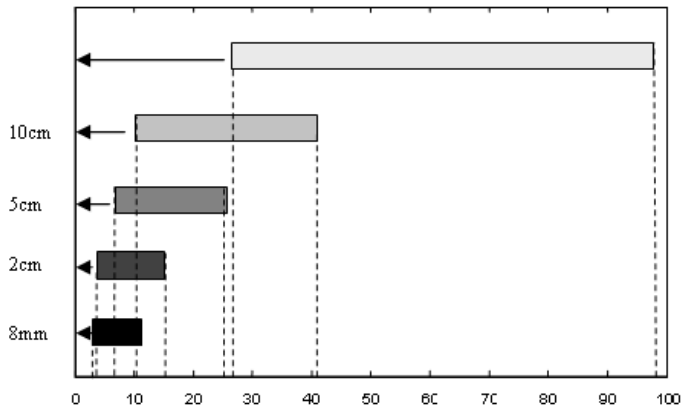

Figure 6. The detectable measuring range of ice thickness of ABMRs with different wavelengths.

The high limit of ice thickness $H_{\max}$ is mainly dependent on the instrumental precision and the penetration depth δ, while the low limit of ice thickness is only dependent on the wavelength of ABMR under the stable circumstance. Fig. 6 shows the measuring rang of ice thickness with $\Delta Tb_{\max} = 1\,\mathrm{K}$ and $\Delta T1\,\mathrm{K}$. It also shows that different frequencies' ABMRs have various measuring ranges of sea-ice thickness. Some of them overlap each other. This proves that ABMR with shorter wavelengths will give more accurate results than those with longer wavelengths if both of them were suitable to detect a certain range of ice thickness.

4. ABMR IN BOHAI SEA ICE THICKNESS DETECTION

When ABMR is applied to detect ice thickness in Bohai Sea, ABMR needs to be associated with the ice thickness in different ice conditions. The ice thickness in Liaodong Bay is the highest in Bohai sea ice. Table 3 listed the ice thickness ranges in different ice conditions [17].

Figure 7 shows the ice thickness range of ABMRs with different frequencies and precisions in Liaodong Bay. It can be found that the ABMRs with the wavelengths of 8 mm and 2 cm and with the precision

Table 3. Ice thickness ranges in different ice conditions in Liaodong bay.

Ice condition	Ice thickness range(cm)
Level-1 ice year	<15
Level-2 ice year	15~25
Level-3 ice year	25~40
Level-4 ice year	40~45
Level-5 ice year	>50

of less than 0.1 K are suitable to detect ice thickness in Level-1 ice year. ABMR with the wavelength of 5 cm and with the precision of lower than 0.001 K is suitable for the ice thickness detection in Level-3 ice year of Bohai Sea. It is also suitable to detect ice thickness in Level 5 ice year if the instrumental precision reaches 0.001 K.

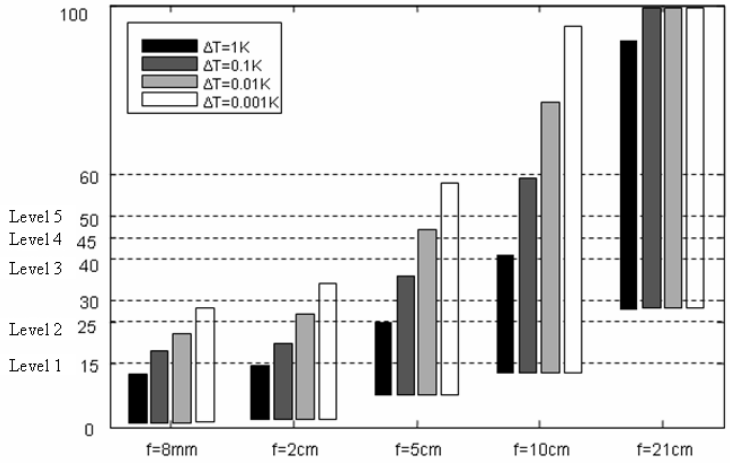

Figure 7. The relation of ice thickness range of ABMR and ice conditions in Liaodong Bay of Bohai Sea.

However, the low limit of Bohai Sea ice thickness reached 7.3 cm. This value is higher than the ice thickness in the period of ice formation as well as ice melting stage in Bohai Sea. In similar, the low limit ice thickness of ABMR with the wavelength of 10 cm is a high value. This is not suitable for ice thickness detection in normal ice years and light ice years in Bohai Sea. The low limit of ice thickness of ABMR with 21 cm wavelength is beyond the ice thickness range in light ice years. In that case, the inversion error is remarkable. Therefore, ABMR with the wavelength of 21 cm is not useful for ice thickness detection in

Bohai Sea.

From the suitable measuring range of ice thickness, a 5 cm wavelength instrument should be selected in heavy ice years in Bohai Sea when thick ice exists. The wavelength of 2 cm or 8 mm ABMR can be used when the ice condition is not more serious than that in normal ice years. According to the former analysis, shorter wavelengths ABMR should be selected because of smaller measurement error [18–24] when both ABMR instruments with different frequencies are suitable for the detection of a certain range of sea ice thickness in Bohai Sea. In addition, the precision of the instrument should be improved the inversion results.

5. SUMMARY AND CONCLUSIONS

We have the following summary and conclusions in Bohai Sea ice detection:

A) The non-linear ice thickness inversion model has the detection scope that is only suitable for a certain range of ice thickness detection. It has not only the maximal detectable ice thickness, but also the minimal detectable sea ice thickness.

B) The maximal detectable ice thickness is mainly dependent on the instrumental precision and the penetration depth, while the minimal detectable ice thickness is independent of instrumental precisions. But it is only related to the change of the instrument wavelengths.

C) The ABMR with shorter wavelengths and a higher precision should be selected when both kinds of ABMR instruments with different frequencies are suitable for the detection of certain range of sea ice thickness in Bohai Sea.

D) The ABMR with the wavelength of 5 cm is suitable for the ice thickness detection in Bohai sea when ice condition is not serious than heavy ice years. ABMRs with 8 mm and 2 cm can be selected in Level-1 and Level-2 ice-condition years with higher detection accuracy than a higher ABMR wavelength (e.g., 10 cm).

ACKNOWLEDGMENT

The authors would like to thank the National High Technology Research and Development Program of China, with the support of "air-born remote sensor integration and applied technique system (No. 2001AA633)". They also thank anonymous reviewers for scientific comments.

REFERENCES

1. Bai, S., Q. D. Liu, H. Li, et al., "Sea ice in the Bohai Sea of China," *Marine Forecasts*, Vol. 16, No. 3, Aug. 1999.
2. Shi, P., S. Ha, Y. Yuan, et al., "The desalinization of Bohai Sea ice and its use value as fresh water resource," *Journal of Natural Resources*, Vol. 17, No. 3, 353–360, 2002.
3. Klein, L. A. and C. T. Swift, "An improved model for the dielectric constant of sea water at microwave frequency," *IEEE Trans Antennas Propag.*, Vol. 25, 104–111, 1977.
4. Shi, Z. F., J. R. Zhang, and K. Zhao, "Improving of microwave remote sensing of sea ice," *Geoscience and Remote Sensing Symposium*, IGARSS, Vol. 3, 1267–1269, 1993.
5. Drucker, R., S. Martin, and R. Moritz, "Observations of ice thickness and frazil ice in the St. Lawrence Island polynya from satellite imagery, upward looking sonar, and salinity/temperature moorings," *J. Geophys. Res.*, Vol. 108, No. C5, 3149, 2003.
6. Martin, S., R. Drucker, R. Kwok, and B. Holt, "Estimation of the thin ice thickness and heat flux for the Chukchi Sea Alaskan coast polynya from SSM/I data," *J. Geophys. Res.*, Vol. 109, 1990–2001, 2004.
7. Martin, S., R. Drucker, R. Kwok, and B. Holt, "Improvements in the estimates of ice thickness and production in the Chukchi Sea polynyas derived from AMSR-E," *J. Geophys. Res.*, Vol. 32, L05505, 2005.
8. Chen, Y., M. Wu, and S. Tan, "Data processing of the airborne remote sensing of sea-ice using a 10 cm microwave radiometer and a 8 mm scanning microwave radiometer," *Ocean Technology*, Vol. 6, No. 4, 12–24, 1987.
9. Liu, X., Y. Z. Hu, and S. Tan, "The research for application of microwave radiometer to the air-borne remote sensing of sea ice," *Journal of Hebei University of Technology*, Vol. 21, No. 3, 1992.
10. Wu, M. Y. and X. Luo, "Study on sea ice microwave radiating propagation model and experiment," *Journal of Remote Sensing*, Vol. 3, No. 1, 16–22, 1999.
11. Guo, F. L., R. Y. Zhao, and W. B. Wang, "Application of passive microwave remote sensing to sea ice thickness measurement," *Journal of Remote Sensing*, Vol. 4, No. 2, 112–117, 2000.
12. Jin, Y. Q., J. R. Zhang, and R. Y. Zhao, "Remote sensing of sea ice by multi-frequency microwave radiometers and numerical modeling of radiative transfer," *Journal of Remote Sensing*, Vol. 7, No. 1, 32–40, Feb. 1992.

13. Bi, D., *Theory of Electromagnetic Field*, Electric Industry Press, Beijing, 1985.
14. Xie, S. S. and Y. J. Xu, *Microwave Remote Sensing Technology and Application*, Electric Industry Press, Beijing, 1987.
15. Comiso, J. C., "Arctic multiyear ice classification and summer ice cover using passive microwave satellite data," *J. Geophys. Res.*, Vol. 95, 13411–13422, 1990.
16. Ulaby, F. T., R. K. Moore, and A. K. Fung, *Microwave Remote Sensing*, Vol. 3, From Theory to Applications, Artech House, 1986.
17. Yang, G. J., *Engineering Ice*, 38, Petroleum Industry Press, Beijing, 2000.
18. Storvold, R., E. Malnes, Y. Larsen, K. A. Hogda, S. E. Hamran, K. Muller, and K. A. Langley, "SAR remote sensing of snow parameters in Norwegian areas-current status and future perspective," *J. Electromagn. Waves Appl.*, Vol. 20, No. 13, 1751–1759, 2006.
19. Mizuno, M., C. Otani, K. Kawase, Y. Kurihara, K. Shindo, Y. Ogawa, and H. Matsuki, "Monitoring the frozen state of freezing media by using millimeter waves," *J. Electromagn. Waves Appl.*, Vol. 20, No. 3, 341–349, 2006.
20. Albert, M. D., T. E. Tan, H. T. Ewe, and H. T. Chuah, "A theoretical and measurement study of sea ice and ice shelf in Antarctica as electrically dense media," *J. Electromagn. Waves Appl.*, Vol. 19, No. 14, 1973–1981, 2005.
21. Mudaliar, S., "On the application of the radiative transfer approach to scattering from a random medium layer with rough boundaries," *J. Electromagn. Waves Appl.*, Vol. 20, No. 13, 1739–1749, 2006.
22. Wang, S., X. Guan, D. Wang, X. Ma, and Y. Su, "Electromagnetic scattering by mixed conducting/dielectric objects using higher-order MOM," *Progress In Electromagnetics Research*, PIER 66, 51–63, 2006.
23. Khalaj-Amirhosseini, M., "Microwave filters using waveguides filled by multi-layer dielectric," *Progress In Electromagnetics Research*, PIER 66, 105–110, 2006.
24. Avdeev, D. B. and A. D. Avdeeva, "A rigorous three-dimensional magnetotelluric inversion," *Progress In Electromagnetics Research*, PIER 62, 41–48, 2006.